Filamentation of ultrashort laser radiation in aerosol

A.A. Zemlyanov and Yu.E. Geints

Institute of Atmospheric Optics,
Siberian Branch of the Russian Academy of Sciences, Tomsk

Received February 22, 2005

We present a numerical study of the filamentation of femtosecond laser pulses in air in the presence of aerosol on the optical path. The effect of a localized absorbing layer that models an aerosol medium on the filament length has been investigated. The dependence of the length of a nonlinear wave guide not only on the optical depth of the aerosol layer, but also on its location on the propagation path has been established for the first time. The length of the filament reaches its maximum when the nonlinear focus of the beam is located behind the aerosol layer and not in front of it.

Introduction

The use of high-power ultrashort laser pulses in atmospheric optics studies is certainly promising from the viewpoint of overcoming the restrictions, traditional for atmospheric propagation, which are imposed on the parameters of laser radiation by thermal nonlinearity and optical breakdown of air [Ref. 1, p. 14].

A laser pulse, passing through an ensemble of particles, undergoes extinction due to scattering and absorption by particles. In the linear mode, the extinction of radiation having passed through an aerosol layer is known to be described by the Bouguer law. As the laser pulse shortens, the process of light scattering by particles becomes nonstationary. Time shift appears in the time profiles of the incident and scattered pulses,[2] and integral characteristics of scattered radiation change.[3]

The high peak intensity of the ultrashort radiation leads to additional nonlinear losses of the light energy due to multiphoton ionization of the particulate matter and light absorption by the generated plasma centers.[4] In addition, even in a medium with the homogeneous phase composition, the ultrashort radiation undergoes strong self-modulation in space and time. In this case, due to the dynamic balance between the Kerr self-focusing, nonlinear multiphoton absorption, and gas ionization, an extended nonlinear wave-guide channel (filament) with a quasicontinuous peak intensity and size is formed. In the atmosphere, the transverse diameter of the filament is usually 100–150 μm for radiation at 800 nm wavelength, while the peak intensity in the filament is $I_0 \approx 10^{13}$–10^{14} W/cm^2 [Refs. 5 and 6]. In this connection the question arises on what how the aerosol medium will modify the regularities of filamentation of the femtosecond radiation in gas?

There are two aspects of this problem. (1) The filament evolution for the light beam, meeting isolated microparticles on its path, and (2) propagation of the filamented radiation through the dense aerosol layer as a whole. As to the influence of isolated particles, there are both experimental[7] and numerical[8] studies, the results of which indicate that the intensity distribution across the light beam is quite highly resistant to the local extinction of its central filamented area by a particle or an absorbing disk screen. This effect was called "filament self-healing" and is explained within the model of dynamic spatial replenishment of the filament energy[9] as the light energy comes from the beam periphery to its axis.

In Ref. 10, this effect was interpreted based on numerical calculations as natural evolution of a spatial soliton at the beam center in the saturable dissipative medium against the background of the Kerr focusing. In any case, the self-recovery of the transverse beam profile after diffraction at an aerosol particle is indicative of the important role of the off-axis areas (photon reservoir) in this process. These areas carry the most fraction of the light energy of the beam and are capable of recovering the filament due to nonlinear focusing.

In this connection, it becomes important to study the influence of aerosol extinction of this photon reservoir on the process of filamentation of the light beam, especially since the most typical situation under real conditions is just the situation, when the whole beam, rather than its central part only, is screened by aerosol, for example, when the radiation propagates through a cloud. It should be noted that Ref. 7 mentioned above has already presented some experimental studies of the case when the filament arising upon the propagation of the femtosecond pulse (wavelength $\lambda_0 = 810$ nm, energy $W_0 = 7$ mJ, duration $t_p = 120$ fs) is blocked by an artificial fog of different density (mean droplet size ~ 2 μm, concentration $\leq 10^6$ cm^{-3}). It was noted that once the radiation has passed through the aerosol chamber, the sharply inhomogeneous transverse beam profile, characteristic of self-focusing, kept up to the fog optical thickness ~ 3.2. In this case, the total energy of the beam at the exit from aerosol decreased exponentially with the increase of the fog optical thickness.

0235-6880/05/04 294-05 $02.00

The first Russian experiments[11] on the propagation of subterrawatt femtosecond pulses of a Ti:sapphire laser ($\lambda_0 = 810$ nm, $W_0 < 17$ mJ, $t_p = 80$ fs) in air with a spatially localized aerosol layer (a jet of water droplets with the rms radius ~ 2.5 μm) have shown that the extinction of the filamented beam by the aerosol layer generally occurs in the quasi-linear mode. It has been noted that the only difference from the mode of linear extinction of the cw radiation is a somewhat higher final extinction coefficient of an optical path for femtosecond pulses. This is obviously connected with additional nonlinear energy losses of the femtosecond beam due to gas ionization and appearance of absorbing centers of optical breakdown inside aerosol particles. It has been also found that the presence of aerosol on the optical path changes neither the number nor the mutual arrangement of the filaments formed.

Thus, it can be believed that the aerosol extinction of a ultrashort laser pulse obeys the same laws as in the case of cw radiation. Consequently, in numerical calculations it is possible to simulate the radiation propagation through an aerosol layer by supplementing the initial equation of light pulse propagation (nonlinear Schrödinger equation) at a given part of the path with a distributed amplitude screen having the absorption coefficient, equal to the coefficient of nonlinear aerosol extinction.

In this paper, such a model is used to study the effect of a localized absorbing layer, simulating an aerosol medium, on the spatial extension of the light filament formed as a result of self-action of femtosecond laser pulses in air. The results of numerical simulation of the light beam filamentation, presented below, indicate that the length of nonlinear wave guide depends not only on the optical density of the aerosol layer, but also on its position on the propagation path. To obtain the maximum filament length, all other conditions being the same, the nonlinear focus of the beam should lie behind the aerosol layer rather than in front of it.

Mathematical formulation of the problem

In the paraxial approximation, the light pulse propagation is usually described by the nonlinear Schrödinger equation for the normalized complex envelope of the electric field of the light wave $U(\mathbf{r}'_\perp, z'; t') = E(\mathbf{r}'_\perp, z'; t')/E_0$ in the coordinate system moving with the group velocity of the pulse v_g (according to designations used in Ref. 12):

$$\left\{\frac{\partial}{\partial z} - \frac{i}{4}\nabla_\perp^2 + i\frac{L_D}{L_{ds}}\frac{\partial^2}{\partial t^2} - ip_{nl}(\mathbf{r}_\perp, z; t)\right\}U(\mathbf{r}_\perp, z; t) + \frac{1}{2}L_D\alpha_a(\mathbf{r}_\perp, z)U(\mathbf{r}_\perp, z; t) = 0, \quad (1)$$

where $r_\perp = r'_\perp/R_0$; $z = z'/L_D$; $t = (t' - z'/v_g)/t_p$ is the current time; t_p is the pulse duration; $L_D = k_0 R_0^2/2$ is the Rayleigh length of the beam; R_0 is the initial beam radius; $k_0 = \omega_0 n_0/c$ is the wave number; ω_0 is the central frequency of laser radiation; $L_{ds} = t_p^2/k''_\omega$ is the dispersion length; $k''_\omega = \partial^2 k/\partial\omega^2 = 0.21$ fs^2/cm is the dispersion of group velocity; p_{nl} is the dimensionless nonlinear polarization of the medium; α_a is the volume coefficient of linear aerosol extinction (the linear gas absorption is neglected).

The equation for the nonlinear polarization of the medium p_{nl} accounts for the effects of the third order in terms of the field: fast (electron) Kerr effect, inertial (time-integral) stimulated Raman scattering at rotational transitions of gas molecules, and radiation absorption and defocusing by plasma formed as a result of gas ionization:

$$p_{nl}(\mathbf{r}_\perp, z; t) = \frac{L_D}{L_K}\left\{(1 - f_R)|U|^2 U + f_R U \int_{-\infty}^{t} R(t - \zeta)|U(\zeta)|^2 d\zeta\right\} - \frac{L_D}{L_{pl}}\left(1 - \frac{i}{\omega_0\tau_c}\right)\rho_e(\mathbf{r}_\perp, z; t)U + i\frac{L_D}{L_{MPA}}|U|^{2(m-1)}U. \quad (2)$$

Here $L_K = c/(\omega_0 n_2 I_0)$ is the length of Kerr nonlinearity ($I_0 = cn_0|E_0|^2/(8\pi)$); $n_2 = 3.2 \cdot 10^{-19}$ cm^2/W is the nonlinear addition to the gas refractive index n_0; f_R is the specific fraction of the inertial Raman scattering in the total change of the nonlinear refractive index (usually it is taken $f_R = 0.5$); $R(\tau - \zeta)$ is the function accounting for the SRS inertia (model of a damped oscillator[13]); $\tau_c = 350$ fs is the characteristic time of electron collision; $L_{MPA} = (\Delta E_i \eta_{MPA}^{(m)} I_0^{m-1})^{-1}$ is the length of the m-photon absorption;

$$L_{pl} = 2L_{MPA}/(\eta_{cas} I_0 t_p n_0^2 \omega_0 \tau_c)$$

is the length of plasma nonlinearity; $\rho_e = N_e/N_{e0}$; where N_e is the concentration of free electrons, $N_{e0} = t_p I_0/(L_{MPA}\Delta E_i)$; $\Delta E_i = 2.3 \cdot 10^{-3}$ fJ is the effective atomic ionization potential of air; $\eta_{MPA}^{(m)}$, η_{cas} are the rates of the multiphoton and cascade gas ionization, respectively.

The change of the normalized concentration of free electrons ρ_e in the field of an ultrashort laser pulse was calculated according to the *Drude* plasma model, ignoring the recombination losses:

$$\frac{\partial\rho_e}{\partial t} = |U|^{2m} + \alpha_{cas}\rho_e|U|^2, \quad (3)$$

where

$$\alpha_{cas} = \frac{L_{MPA}}{L_{pl}}\frac{2}{n_0^2\omega_0\tau_c}$$

is the coefficient of cascade ionization.

The initial spatiotemporal profile of the laser beam was specified as a combination of the Gaussian functions:

$$U(x,y,z=0;t)=\exp\left\{-\left(\frac{(x^2+y^2)}{2}\right)\left(1+i\frac{k_0R_0^2}{F}\right)\right\}\exp\left\{-\frac{t^2}{2}\right\}, \quad (4)$$

where F is the initial radius of curvature of the wave front.

Results of numerical experiments

The problem (1)–(4) was solved numerically in the four-dimensional (3D + 1) space using the technique of splitting the initial problem into the parts according to physical factors, and the beam diffraction and dispersion were calculated in the domain of spatial and temporal frequencies, while nonlinear self-action was calculated in the signal space. The adaptive correction of the grid step was applied along the propagation variable (z). The equation (3) was solved numerically by the fourth-order Runge–Kutta method.

Figure 1 shows the two-dimensional energy density profile of the laser beam in the x–z coordinates for the beam propagating in clear and nonturbid air and in the presence of an aerosol layer at different sections of the optical path: before the filamentation zone and inside the filament formed due to self-focusing. The parameters of laser radiation corresponded to the pulse with $\lambda_0 = 800$ nm, $t_p = 80$ fs, $R_0 = 1.5$ mm, $F = 0.6L_D$. The pulse energy was $W_0 \sim 8$ mJ, and the initial peak power P_0 15 times exceeded the critical self-focusing power ($P_{cr} = 3.2$ GW). The aerosol was simulated by an absorbing screen, intercepting the whole beam, with the length $d_a = 0.05L_D$ and the optical thickness $\tau_0 = 1$.

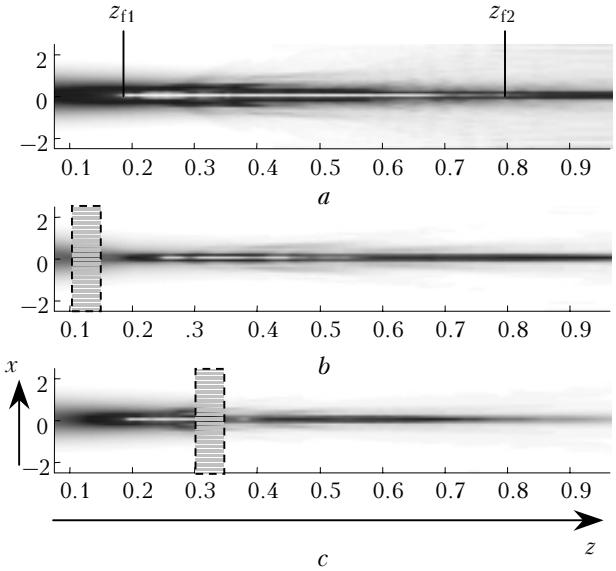

Fig. 1. x–z energy density (rel. units) profile of the laser beam ($P_0/P_{cr} = 15$), propagating in air without aerosol (*a*) and with aerosol layer (*b*, *c*) at $\tau_0 = 1$. The position of the aerosol layer is shown by the rectangle, the filament is shown by the light band near the axis.

It is seen from Fig. 1 that, at the parameters used in the numerical experiment, the zone of the increased energy density with the diameter $\sim 0.1R_0$ is formed on the laser beam axis, and the trace of this zone along the propagation path resembles a filament. In the clear air, the filament appears much earlier than the diffraction focus of the beam ($z_{f1} \approx 0.2\,L_D < F/L_D$) and has the mean length $L_f = (z_{f2} - z_{f1}) \sim 0.6L_D$. The concentration of free electrons N_e, formed mostly due to the multiphoton ionization of air molecules, is rather high in the filament zone (Fig. 2).

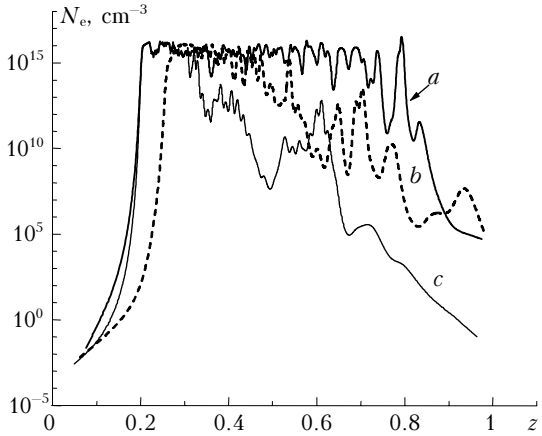

Fig. 2. Density of electrons in plasma on the laser beam axis along the propagation path for the three cases considered in Fig. 1.

The values of N_e vary near the level $\sim 10^{16}$ cm^{-3}, whereas the dynamic balance is established between the Kerr focusing of consecutive time layers of the laser pulse and the defocusing effect of the plasma nonlinearity.

Our numerical calculations (the results are omitted in this paper) with the "off" dispersion term in Eq. (1) have confirmed the decisive role of material dispersion of the medium in distortion of the filament stability and in the following diffraction dissipation of the filament, which was earlier noted by some authors [Refs. 14 and 15]. Thus, the light filament exists until the dispersion break of the temporal profile of the initial pulse into a series of much shorter pulses with the characteristic duration $\sim 0.1t_p$, occurring against the background of the strong nonlinear phase self-modulation, worsens its coherent properties. As a result of this process, the initially quasi-Gaussian (in time) filament transforms into a structure consisting of a series spatially and temporally separated, weakly bound individual pulses, undergoing much stronger dispersion blooming than the initial pulse.

Let us now return to the energy profiles shown in Fig. 1. As can be seen from Figs. 1*b* and *c*, when the absorbing screen, simulating the aerosol layer, is set on the beam path, the filament length decreases. The effect of the aerosol on the filament dynamics

appears to be different depending on the position of the aerosol layer on the path, the extinction being the same.

If the aerosol layer is placed before the nonlinear focus of the beam (Fig. 1*b*), the position of this focus shifts, because the peak power of the beam P_0 decreases, and $z_{f1} \sim (P/P_{cr})^{-1}$ according to Ref. 16. In addition, the radiation energy loss after the passage through the absorbing screen becomes critical for further maintenance of the filament due to the dynamic influx of the light energy from the beam periphery to the axis, which shortens the coordinate z_{f2}.

However, the strongest effect on the filament length is observed in the case, when the already filamented beam is incident on the aerosol layer (see Fig. 1*c*). The aerosol optical thickness $\tau_0 = 1$ appear sufficient to block the filament. As can be seen from Fig. 2 (curve *c*), at the rear boundary of the aerosol layer, the density of the plasma, formed on the beam axis, decreases sharply to the level $N_e \sim 10^{11}$ cm^{-3}. Then small-scale oscillations of N_e occur due to the nonlinear lens, formed at the beam periphery, but no spatially stable structure is formed near the beam axis.

This result again points to the dispersion mechanism of collapse of the axial wave-guide channel (in the range of radiation parameters used in our calculations), because the main difference between the versions shown in Figs. 1*b* and *c* is only the spatiotemporal intensity profile on the beam axis in the aerosol zone. In the first case it is close to the Gaussian one, while in the second case it is strongly fragmented in time.

Figure 3 illustrates the mentioned effect of filament self-healing after the passage through the aerosol layer. The parameters of calculation here were the same as in Fig. 1*c*, but the length of the absorbing layer was fivefold shorter with the optical thickness kept at the level $\tau_0 = 1$.

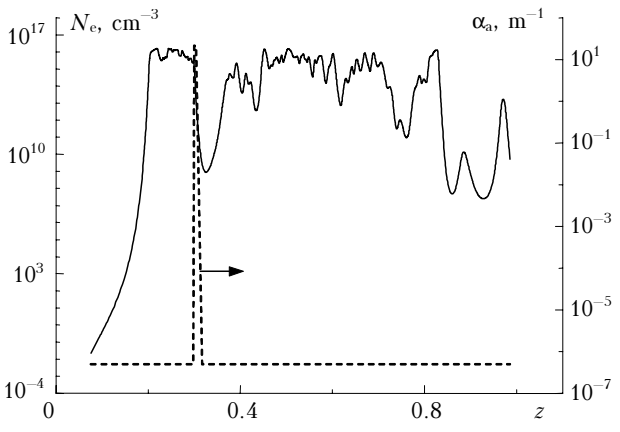

Fig. 3. Effect of filament self-healing: concentration of electrons in plasma on the laser beam axis ($P_0/P_{cr} = 15$) and volume coefficient of linear absorption α_a along the optical path.

As can be seen, after the exit from the aerosol layer, the axial, spatially localized zone of the increased beam intensity first disappears, simultaneously with the decrease of the free electron concentration (Fig. 1*b*). Then, however, the filaments re-form due to the Kerr self-focusing of the off-axis beam zones, and the further filament evolution is similar to that in the case of the nonturbid atmosphere (Fig. 1*a*), although the filament itself losses stability (becomes broken) along the propagation direction.

The influence of the aerosol extinction on the spatial length of the filament is illustrated by Fig. 4. Three versions with the different initial pulse energy and, correspondingly, the different ratio (P_0/P_{cr}) are considered. The filament length in numerical calculations was determined as the concentration of free electrons on the beam axis achieved the value $N_{ef} = 10^{15}$ cm^{-3}, which corresponds to the experimental data.[17] Because the filament was broken along the path, the right filament boundary z_{f2} was taken equal to the value of the variable z, after which the level N_{ef} already was not achieved. The aerosol layer was set before the nonlinear focus of the beam.

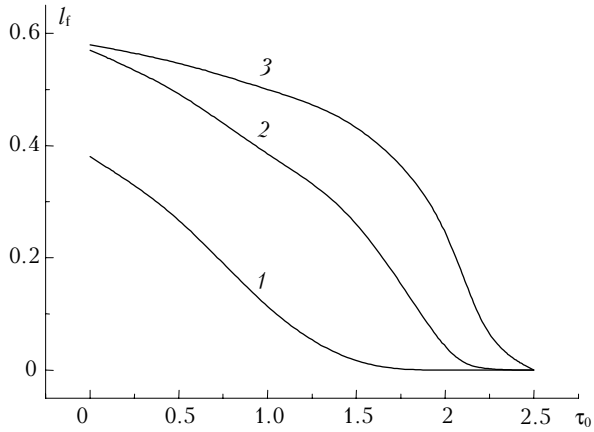

Fig. 4. Relative length of the light filament $l_f = L_f/L_D$ as a function of the optical thickness of the aerosol layer at the different peak power of the initial pulse: $P_0/P_{cr} = 6$ (*1*), 15 (*2*), and 31 (*3*).

It can be seen from Fig. 4 that, as the optical density of the aerosol increases, the filament length shortens and even vanish. The limiting optical thickness, at which the filament is still formed, depends on the initial radiation power and corresponds to the criterion of self-focusing in the presence of extinction[18]: $P_0 \exp\{-\tau_0\} > P_{cr}$. Note that the character of change of the relative filament length $l_f = L_f/L_D$ as a function of τ_0 is also different at different P_0.

At the initial beam power much higher than the critical one ($P_0/P_{cr} = 31$), the length of the formed filament weakly depends on the optical thickness of aerosol up to $\tau_0 \cong 1.6$, which indicates that the central zone of the beam dynamically receives the

energy from the beam periphery. Then, however, l_f decreases rather sharply and quickly achieves zero level. For less powerful beams ($P_0/P_{cr} = 6$), as can be seen from Fig. 4, the process of the transverse energy transfer is less pronounced, and l_f decreases smoothly and almost linearly.

Conclusions

Thus, the numerical simulation of self-action of femtosecond laser pulses in air with an aerosol layer has shown that the increase of the optical thickness of aerosol leads to shorter length of the filament formed. In addition, the filament length depends on the position of the aerosol layer on the propagation path and its geometric thickness (at the unchanged optical thickness). The filament length is maximum, if the nonlinear focus of the beam is located behind the aerosol layer rather than in front of it.

Under certain conditions (aerosol layers thin as compared with the diffraction length of the initial beam), the nonlinear wave-guide channel (filament), formed on the beam axis because of the beam self-focusing, can recover after breaking caused by its passage through an optically dense attenuating layer. After the filament recovery, its further evolution differs only slightly from the case of the non-attenuating layer.

The physical cause for this effect is that the filament recovery after the attenuating layer occurs due to the dynamical replenishment of energy in the central part of the beam from the beam periphery owing to the self-focusing process.

Acknowledgments

This work was supported, in part, by the Russian Foundation for Basic Research (Grant No. 03-05-64228), CRDF (Grant RP0-1390-TO-03), the Russian Academy of Sciences (Program "Femtosecond Optics and Physics of Superstrong Laser Fields"), Presidium SB RAS (Combined Integration Project No. 12), and the Division of Physical Sciences of RAS (Project 2.9).

References

1. V.E. Zuev, A.A. Zemlyanov, and Yu.D. Kopytin, *Nonlinear Optics of the Atmosphere* (Gidrometeoizdat, Leningrad, 1989), 256 pp.
2. A.A. Zemlyanov and Yu.E. Geints, Atmos. Oceanic Opt. **15**, No. 8, 619–621 (2002).
3. K.S. Shifrin and I.G. Zolotov, Appl. Opt. **34**, No. 3, 552–558 (1995).
4. F. Courvoisier, V. Boutou, C. Favre, S.C. Hill, and J.-P. Wolf, Opt. Lett. **28**, No. 3, 206–208 (2003).
5. E.T.J. Nibbering, P.F. Curley, G. Grillon, B.S. Prade, M.A. Franco, F. Salin, and A. Mysyrowicz, Opt. Lett. **21**, No. 1, 62–64 (1996).
6. W. Liu, S.A. Hosseini, Q. Luo, B. Ferland, S.L. Chin, O.G. Kosareva, N.A. Panov, and V.P. Kandidov, New J. Phys. **6**, No. 6, 1–22 (2003).
7. F. Courvoisier, V. Boutou, J. Kasparian, E. Salmon, G. Mejean, J. Yu, and J.-P. Wolf, Appl. Phys. Lett. **83**, No. 2, 213–215 (2003).
8. M. Kolesik and J. Moloney, Opt. Lett. **29**, No. 6, 590–592 (2004).
9. M. Mlejnek, M. Kolesik, E.M. Wright, and J.V. Moloney, Math. Comput. Simul. **56**, 563–570 (2001).
10. S. Skupin, L. Berge, U. Peschel, and F. Lederer, Phys. Rev. Lett. **93**, No. 2, 023901-1–023901-1 (2004).
11. N.N. Bochkarev, A.A. Zemlyanov, Al.A. Zemlyanov, A.M. Kabanov, D.V. Kartashov, A.V. Kirsanov, G.G. Matvienko, and A.N. Stepanov, Atmos. Oceanic Opt. **17**, No. 12, 861–864 (2004).
12. A.L. Gaeta, Phys. Rev. Lett. **84**, No. 16, 3582–3585 (2000).
13. M. Kolesik, J.V. Moloney, and E.M. Wright, arXiv:physics/0101073.v1.2001.
14. Dubietis, E. Gaizauskas, G. Tamosauskas, and P.D. Trapani, arXiv:physics/0311072 v1. 2003.
15. M. Kolesik, E.M. Wright, and J.V. Moloney, arXiv:physics/0311021 v1. 2003.
16. S.N. Vlasov and V.I. Talanov, *Wave Self-Focusing* (IAP RAS, Nizhnii Novgorod, 1997), 200 pp.
17. J. Kasparian, R. Sauerbrey, and S.L. Chin, Appl. Phys. B **71**, 877–879 (2000).
18. G. Fibich, SIAM J. Appl. Math. **61**, No. 5, 1680–1705 (2001).